

FINE PHENOMENA IN THE EPR SPECTRA OF THE HOLE-LIKE
PARAMAGNETIC CENTRE IN CYTOSINE HYDROCHLORIDE

DUBRAVKA KRILOV^a, KREŠIMIR SANKOVIĆ^c, TATJANA PRANJIĆ-PETROVIĆ^b
and JANKO N. HERAK^c

^a*School of Medicine and* ^c*Faculty of Pharmacy and Biochemistry, University of Zagreb,
Zagreb, Croatia*

^b*School of Medicine, University of Rijeka, Rijeka, Croatia*

Dedicated to Professor Mladen Paić on the occasion of his 90th birthday

Received 24 July 1995

UDC 538.955

PACS 76.30.-v

The fine phenomena in the EPR spectra of the hole-like paramagnetic centre formed in cytosine(thiocytosine)-HCl crystals upon irradiation are studied with EPR spectroscopy. The spin Hamiltonian including the electronic Zeeman term, hyperfine coupling, quadrupole coupling and the nuclear Zeeman term has been used in the second-order perturbation treatment for the interpretation of the experimental observations. It is shown that the quadrupolar term causes a detectable shift of the EPR lines and also induces the “forbidden” transitions. From the shift of the “allowed” transitions and the positions of the “forbidden” transitions, the chlorine quadrupolar coupling tensor \hat{P} , has been determined.

1. Introduction

It has been well established that the transfer and trapping of the excess energy deposited by ionizing radiation in nucleic acids and the related model systems, strongly depend on the presence of thioanalogs as substitutional impurities in the irradiated systems [1-6]. Thiocytosine and thioguanine, present in concentrations

less than 1% of that of cytosine or guanine, stabilize the damage predominantly in a form of sulfur-centered radicals. The crystals composed of hydrochlorinated bases, cytosine or guanine, with traces of thiocytosine or thioguanine as substitutional impurities, when irradiated with γ - or X-rays, exhibit the paramagnetic species with the unpaired electron shared by sulfur and chlorine. It has been shown that the paramagnetic centre is an electron-deficient, hole-like species [6].

The dominating spectral features are determined by an anisotropic g -factor and an anisotropic quartet hyperfine splitting, due to the coupling of a ^{35}Cl nucleus ($I = 3/2$), with natural abundance of about 75%, along with a less intensive EPR spectrum of the same characteristics, brought about by the less abundant Cl isotope, ^{37}Cl ($I = 3/2$, 25% natural abundance). The spectra are quite well understood in terms of the spin Hamiltonian consisting of the large electronic Zeeman term and a smaller, perturbing hyperfine coupling term. The first-order perturbation treatment is adequate for understanding of most of the observed phenomena [4]. However, at certain orientations of the crystal in the magnetic field of the spectrometer, not only the quartet pattern behaves as predicted, but also additional, "forbidden" transitions occur. In order to understand such phenomena, a more complete spin Hamiltonian and a more precise treatment should be used.

In the present work, we describe the fine phenomena for the hole-like paramagnetic centre in irradiated cytosine hydrochloride, with thiocytosine as impurity. It will be shown that some of the spectroscopic features could not be explained if quadrupolar interaction and the nuclear Zeeman term are ignored, in spite of the fact that these terms are very small.

2. Experimental

The crystals of cytosine hydrochloride, with thiocytosine as a substitutional impurity, designated as C(TC)HCl, were grown by evaporation of the solution of cytosine (with the traces of thiocytosine) in hydrochloric acid. Typically, 1% of thiocytosine is added to cytosine before dissolving the powder in HCl. Actual concentrations of thiocytosine were measured by particle-induced X-ray emission (PIXE) [7]. The ratio of thiocytosine to cytosine was found to be 0.006 ($\pm 30\%$). Single crystal of cytosine hydrochloride (and also of C(TC)HCl) is monoclinic with the space group $P2_1/n$, with $a = 832$, $b = 683$, $c = 1104$ pm and $\beta = 96.7^\circ$ [8]. There are four molecules in the unit cell, two of them magnetically distinct. The crystal planes were identified by the reflection of the laser beam from a crystal mounted on a goniometer.

For irradiation and EPR measurements, the crystals were mounted on metal rods in desired orientations. A weak EPR signal originating from irradiated glue could not be avoided. The crystals were irradiated at 77 K, using a strong ^{60}Co source. The dose rate was about 10 kGy h^{-1} and the total dose about 40 kGy. The measurements were made at 77 K with a Varian E-109 spectrometer, equipped with a unit for digital signal recording (Scientific Software Services). For the analysis of the data, the orthogonal a^* , b , c crystallographic system of axes was used.

3. Results

The representative EPR spectra of the hole-like paramagnetic centre in C(TC)HCl are shown in Fig. 1. Spectrum a) is recorded for the magnetic field, \mathbf{B} , in the c direction, $\mathbf{B}||c$, and spectrum b) for $\mathbf{B} \perp b$, 12° from the $\mathbf{B}||b$ direction.

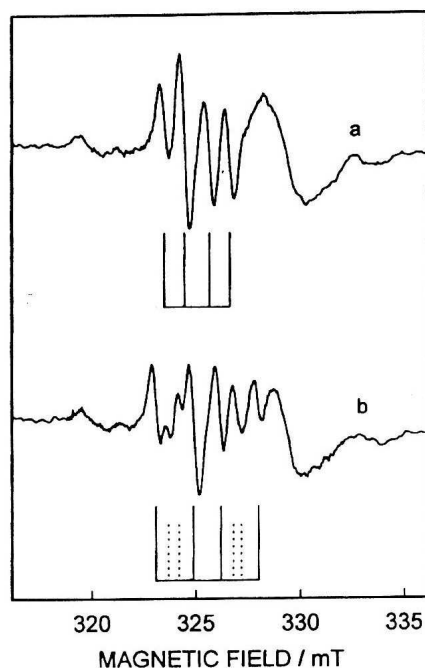


Fig. 1. EPR spectra (first derivative curves) of the irradiated single crystal of C(TC)HCl, for two different orientations in the $\mathbf{B} \perp b$ plane (for $\mathbf{B}||c$ and $\mathbf{B} \perp b$, 12° from the c axis, respectively). The crystals were irradiated at 77 K, and measured at 77 K at microwave frequency of 9.250 GHz, with the microwave power of 5 mW. The solid bars under the spectra indicate the positions of the first-order resonance lines for species A containing the ^{35}Cl isotope. The dashed bars indicate the positions of the second-order resonance lines.

In both of these crystal orientations the crystal symmetry makes all the molecules magnetically equivalent. The EPR spectra clearly indicate the presence of more than one paramagnetic species. It is already known that there are two distinct hole-like centres, named A and B, and a signal at $g \approx 2.003$ brought about by the defects in the host lattice (not associated with thio-impurities) and the unavoidable radicals associated with the irradiated glue. In the present report we deal only with the quartet patterns of centre A, indicated by the bars in Fig. 1. For the orientations where the hyperfine splittings are large, the coupling of both Cl isotopes, ^{35}Cl and ^{37}Cl , is clearly discriminated, the latter isotope giving smaller

intensity. The spectra differ in the line splittings and in the total line spread by about 20%, as a consequence of the different nuclear magnetic moments of the two chlorine isotopes. In the crystal orientations where the hyperfine coupling is small, as depicted in both tracings in Fig. 1, the weaker signal, associated with ^{37}Cl is not clearly discriminated, because the differences between the two spectra are smaller than the line-width. In the lower spectrum in Fig. 1, the additional lines associated with centre A, indicated by the dashed bars under the spectra, are clearly seen. These are the “forbidden” transitions that appear only for certain crystal orientations. We analysed in detail the “regular” and the “extra” EPR lines (the splittings and relative intensities) only in the $\mathbf{B} \perp b$ plane. The “forbidden” transitions are expected to be observable also in the $\mathbf{B} \perp a$ plane. However, in that plane there are two magnetically nonequivalent sites and the spectra are too complex for a precise analysis. Actually, in the present work only the stronger signal brought about by the more abundant chlorine isotope, ^{35}Cl , is analysed.

For the analysis, we use the following spin Hamiltonian:

$$H = \beta \tilde{\mathbf{S}} \hat{\mathbf{g}} \mathbf{B} + \hat{\mathbf{A}} \mathbf{S} - g_n \beta_n \tilde{\mathbf{I}} \mathbf{B} + \tilde{\mathbf{I}} \hat{\mathbf{P}} \mathbf{I}. \quad (1)$$

The first term is the electron Zeeman term, in which β is the Bohr magneton and $\hat{\mathbf{g}}$ the “g factor” (actually a tensor). The second term represents the hyperfine coupling of the unpaired electron with a Cl nucleus, $\hat{\mathbf{A}}$ being the hyperfine coupling tensor. The second term is the nuclear Zeeman term with the nuclear “g-factor” g_n and the nuclear magneton β_n . The last term is the quadrupolar coupling. Here $\hat{\mathbf{P}}$ stands for the quadrupolar tensor. The energy states and the transitions could be calculated using the electron Zeeman term as a dominating term and the perturbation of the remaining terms to the second order. We essentially use the general procedure derived by Iwasaki [9].

The energy levels defined by the electron state M_S and the nuclear state M_I are:

$$\begin{aligned} E(M_S, M_I) = & g\beta B M_S + K(M_S) M_I - \frac{1}{2} (\tilde{\mathbf{k}} \hat{\mathbf{P}} \mathbf{k} [I(I+1) - 3M_I^2] + \\ & + \frac{1}{2g\beta B} \left\{ |A_1|^2 M_S M_I^2 - A_2 [S(S+1) - M_S^2] M_I + \frac{1}{2} A_3 M_S [I(I+1) - M_I^2] \right\} - \\ & - \frac{1}{2K(M_S)} \left\{ |P_1|^2 (M_S) M_I [4I(I+1) - 8M_I^2 - 1] \right. \\ & \left. - \frac{1}{4} |P_2|^2 (M_S) M_I [2I(I+1) - 2M_I^2 - 1] \right\} \end{aligned} \quad (2)$$

where

$$g^2 = \tilde{\mathbf{b}} \hat{\mathbf{g}} \mathbf{g} \mathbf{b}$$

$$\hat{K}(M_S) = (\hat{\mathbf{A}} \hat{\mathbf{G}} / g) M_S - g_n \beta_n B \mathbf{E},$$

$$K^2(M_S) = \tilde{\mathbf{b}} \hat{\tilde{\mathbf{K}}}(M_S) \tilde{\mathbf{K}}(M_S) \mathbf{b}$$

$$|P_1|^2(M_S) = \tilde{\mathbf{k}}(M_S) \hat{\mathbf{P}}^2 \mathbf{k}(M_S) - (\tilde{\mathbf{k}}(M_S) \hat{\mathbf{P}} \mathbf{k}(M_S))^2,$$

$$|P_2|^2(M_S) = 2\text{Tr} \hat{\mathbf{P}}^2 + (\tilde{\mathbf{k}}(M_S) \hat{\mathbf{P}} \mathbf{k}(M_S))^2 - 4(\tilde{\mathbf{k}}(M_S) \hat{\mathbf{P}}^2 \mathbf{k}(M_S))$$

Thus, the energy for any spin state can be expressed in terms of the $\hat{\mathbf{g}} \hat{\mathbf{A}}$ and $\hat{\mathbf{P}}$ tensors and $g_n \beta_n B$ as a function of the external magnetic field in direction \mathbf{b} with respect to the crystal coordinate axes.

The fourth term at right in Eq. (2) is neglected, because its contribution is less than 0.01 mT. That could not be measured. The nuclear Zeeman term is also small (about 0.05 mT), but it is not neglected because it introduces the asymmetry in the second-order spectra that could be observed.

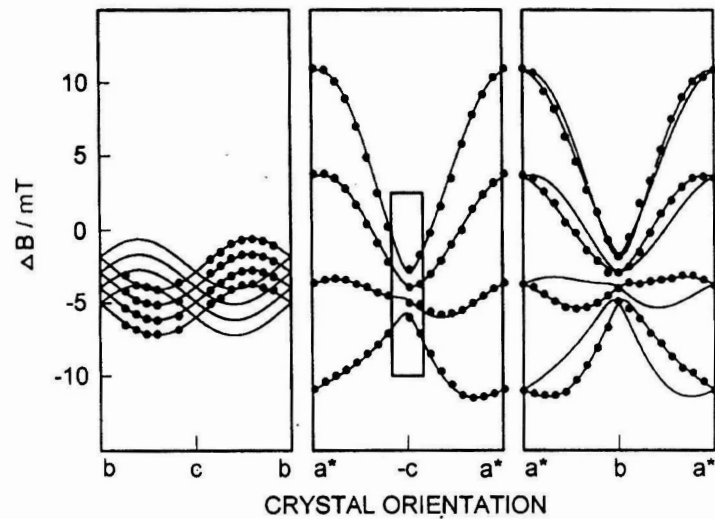


Fig. 2. Angular variation of the positions of the EPR lines for the three reference planes. The dots represent the experimental points and the curves are theoretically reproduced within the first-order approximation. The ordinate axis expresses the deviation of the line positions from a standard position at $g = 2.0036$. The rectangle in the middle panel indicates the region most sensitive to the quadrupolar interactions.

The first-order or “allowed” transitions are defined by $\Delta M_S = \pm 1$ and $\Delta M_I = 0$, giving rise to the quartet pattern with almost equidistant lines for most crystal orientations. In certain orientations the separation between the lines differs significantly. Figure 2 shows the observed angular variation of the quartet lines in the three mutually perpendicular planes. The full lines in the figure represent the predicted behaviour within the first-order treatment, neglecting the quadrupolar term

and the nuclear Zeeman term. The fit is good, except for the crystal orientations where the hyperfine splittings are small. We made a special effort to measure precisely the line positions in the $\mathbf{B} \perp b$ plane, close to $\mathbf{B}||c$, the region marked by the rectangle in the middle panel in Fig. 2. The data for that region are separately shown in Fig. 3. The irregularities, not predicted in the first-order treatment, are nicely seen. Moreover, the “forbidden” transitions, indicated by the triangles for each crystal orientation, are present. The “forbidden” transitions are defined by $\Delta M_S = \pm 1$, $\Delta M_I = \pm 1$. The intensities of these lines vary significantly when crystal orientation in the magnetic field is changed.

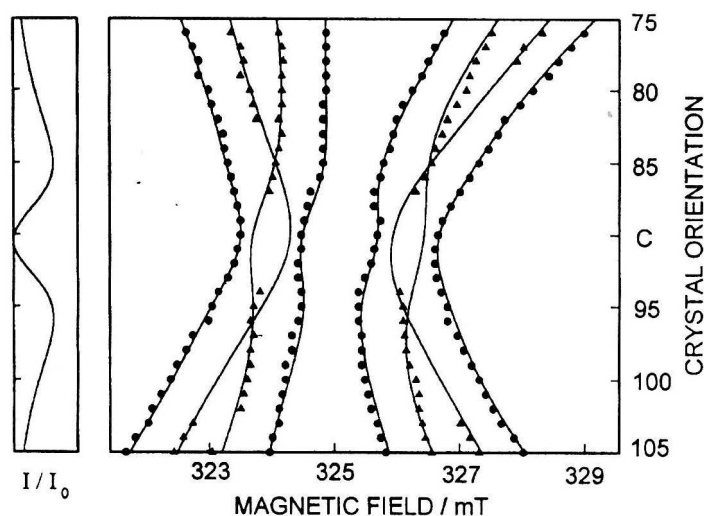


Fig. 3. Angular variation of the positions of the EPR lines in a selected range of orientations in the $\mathbf{B} \perp b$ plane. The circles indicate the position of the first-order transitions and the triangles the measured second-order lines. The full curves show the angular variation theoretically reproduced with the data in Table 1. The side panel shows the relative intensities of the “forbidden” transitions, I/I_0 as a function of the crystal orientation.

Probability of the transition between the $|M_S, M_I(M_S) \rangle$ and $|M'_S, M'_I(M'_S) \rangle$ states is:

$$\begin{aligned}
 I &\sim | \langle M_S, M_I(M_S) | \beta B_1 \tilde{\mathbf{S}} \hat{\mathbf{g}} \mathbf{b}_1 | M'_S, M'_I(M'_S) \rangle |^2 \\
 &= \beta^2 B_1^2 |G|^2 | \langle M_S | S_I | M'_S \rangle |^2 | \langle M_I(M_S) | M'_I(M'_S) \rangle |^2 \quad (3)
 \end{aligned}$$

where

$$|G|^2 = (\tilde{\mathbf{b}}_1 \hat{\mathbf{g}} \mathbf{b}_1) - \frac{1}{g^2} (\tilde{\mathbf{b}}_1 \hat{\mathbf{g}} \hat{\mathbf{g}} \mathbf{b}_1)^2$$

and $2 B_1$ and \mathbf{b}_1 are the strength and the direction of the oscillating magnetic field, respectively.

The intensity of the spin “forbidden” transitions, arising from the quadrupole interaction, relative to the first-order (“allowed”) transitions, $|M_S, k \pm 1/2 \rangle \leftrightarrow |M_S - 1, k \mp 1/2 \rangle$ are:

$$\frac{I}{I_0} = \frac{4k^2 \left[\left(I + \frac{1}{2} \right)^2 - k^2 \right] |P_1|^2}{[2KM_S(M_S - 1)]^2}. \quad (4)$$

Here k takes on the values $(I - 1/2), (I - 3/2), \dots, -(I - 1/2)$. For simplicity, for the calculations of intensity, Eq. (4), the nuclear Zeeman term is neglected.

There are also $\Delta M_S = \pm 1, \Delta M_I = \pm 2$ transitions, not observed in our experiments.

TABLE 1.

Summary of the EPR tensor elements. The hyperfine and quadrupole couplings are expressed in mT.

Tensor	Principal values	Eigenvectors		
		$\langle a^* \rangle$	$\langle b \rangle$	$\langle c \rangle$
g	2.0021	0.975	0.158	-0.155
	2.0174	0.030	0.790	-0.612
	2.0416	0.216	0.592	0.773
A(^{35}Cl)	7.25	0.999	0.049	-0.004
	0.93	-0.047	0.916	-0.399
	0.96	-0.015	0.398	0.917
P	0.180	0.999	0.049	-0.004
	-0.090	-0.047	0.916	-0.399
	-0.090	-0.015	0.398	0.917

The procedure for the determination of the three tensors, $\hat{\mathbf{g}}$, $\hat{\mathbf{A}}$ and $\hat{\mathbf{P}}$, is as follows. From Eq. (2), one can see that the g -factor for each crystal orientation can be deduced directly from the line positions, independently of $\hat{\mathbf{A}}$ or $\hat{\mathbf{P}}$. Then the principal elements of $\hat{\mathbf{g}}$ are determined in a standard way. In contrast, $\hat{\mathbf{A}}$ and $\hat{\mathbf{P}}$ have to be deduced simultaneously by fitting the theoretically derived curve to the experimental data. We rather adopted the following, simplified procedure. First, we deduce the $\hat{\mathbf{A}}$ tensor in the first-order, already standard procedure. Then the $\hat{\mathbf{P}}$ tensor (smaller than $\hat{\mathbf{A}}$) is introduced as a trial tensor and $\hat{\mathbf{A}}$ modified to fit best the experimental points for the crystal orientations shown in Fig. 3. In that

procedure, we used the fact that in most cases the $\hat{\mathbf{A}}$ and $\hat{\mathbf{P}}$ tensors are coaxial and $\hat{\mathbf{P}}$ is axially symmetric [10,11]. The fit was very sensitive to the choice of the parameters. The best fit was attained for the tensor parameters listed in Table 1. The values for $\hat{\mathbf{g}}$ and $\hat{\mathbf{A}}$ are essentially the same as earlier determined [4] in a simpler procedure. The best estimate of the values for $\hat{\mathbf{P}}$ are 0.180, -0.090 and 0.090 mT (± 0.005 mT), the tensor being coaxial with the $\hat{\mathbf{A}}$ tensor. With these parameters, the second-order transitions are predicted theoretically and compared with the observed transitions (Fig. 3). The fit is very good.

By knowing the three tensors, the relative intensity of the second-order transitions, induced by the quadrupole term, could be calculated from Eq. (3). The calculated relative intensities for the indicated section of the $\mathbf{B} \perp b$ plane are shown on the side panel in Fig. 3. As seen, the “forbidden” transitions are expected to be observed in the direction close to $\mathbf{B} \parallel c$, but not exactly in that direction. Note the lack of the extra lines for $\mathbf{B} \parallel c$, tracing a) in Fig. 1.

4. Discussion

It has been shown [4-6] that the hole-like paramagnetic centre in hydrochlorinated purine or pyrimidine systems, with the thioanalogs of the bases as impurities is associated with the unpaired electron shared by the S atom of the impurity and a neighbouring Cl. The proposed structure of the centre is shown in Fig. 4. The coupling nuclei (^{35}Cl and ^{37}Cl) have spin $I > 1/2$ and hence an electron quadrupole, that interacts with the unpaired electron via the nuclear spin. The quadrupolar term introduces very little perturbation in the normal EPR transitions. The effect is observed only occasionally. More important effect of the quadrupolar term in the spin Hamiltonian is the induction of the “forbidden” transitions. Very precise measurements give the information on both the shifts of the regular, “allowed” transitions and the appearance of the “forbidden” transitions. We have shown that the quadrupolar term is small in comparison to the hyperfine coupling term. The values deduced here (0.180, -0.090 and -0.090 mT) are much smaller than the line width. However, from the “forbidden” lines, and even the shift of the “regular” lines, $\hat{\mathbf{P}}$ could be evaluated (See Fig. 3). Inclusion of the nuclear Zeeman term is responsible for the slight asymmetry of the EPR spectra, in particular the different spacing between the two low-field and the two high-field “forbidden” lines.

The deduced values for $\hat{\mathbf{P}}$ are by about a factor of two smaller than the values anticipated from the analysis of the powder spectra [4]. It is quite clear that the present, single crystal data are more reliable. The present values are also smaller than the quadrupolar term derived in a related radical with a Cl atom covalently bound to the carbon atom with the unpaired electron [12]. That difference is not surprising since the quadrupolar term, $H = \hat{\mathbf{I}}\hat{\mathbf{P}}\mathbf{I}$, contains the quadrupolar coupling constant $eQ\partial^2V/\partial x^2$ that depends strongly on the gradient of the electric field, which is obviously different in the two cases.

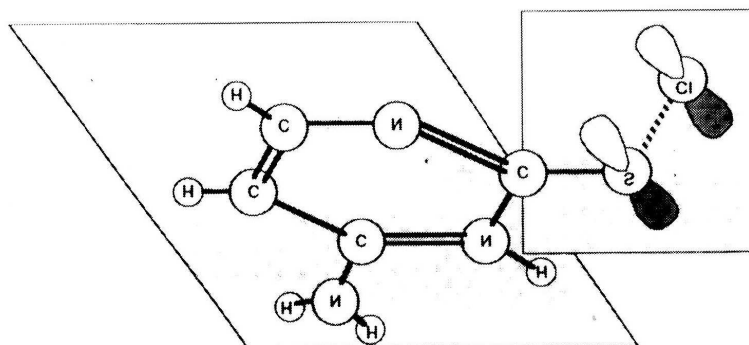


Fig. 4. The model of the hole-like paramagnetic centre.

The present analysis shows that, although in principle it is possible to determine the quadrupolar term arising from the chlorine nuclei from the shift of the first-order transition lines, the procedure is much more reliable if the “forbidden” transitions are utilized. The shift of the first-order lines is small, sometimes almost not detected, particularly if the lines are overlapped by other resonances. On the other hand, the second-order lines are often well expressed and their mere appearance gives sufficient information for the \hat{P} tensor determination. The best situation is if both types of information are used, as in the present study.

References

- 1) K. Sanković, D. Krilov and J. N. Herak, *J. Molec. Structure* **190** (1988) 177;
- 2) J. N. Herak and J. Hüttermann, *Int. J. Radiat. Biol.* **60** (1991) 423;
- 3) K. Sanković, D. Krilov and J. N. Herak, *Radiat. Res.* **128** (1991) 119;
- 4) J. N. Herak, K. Sanković and J. Hüttermann, *Int. J. Radiat. Biol.* **66** (1994) 3;
- 5) J. N. Herak, K. Sanković, D. Krilov and J. Hüttermann, *Radiat. Res.*, (in press);
- 6) J. N. Herak, K. Sanković, M. Jakšić and J. Hüttermann, *Radiat. Res.* (in press);
- 7) S. A. E. Johansson and J. L. Campbell, *PIXE - a Novel Technique for Elemental Analysis*, John Wiley&Sons, Chichester, U.K., 1988;
- 8) N. S. Mandel, *Acta Cryst.* **B33** (1977) 1079;
- 9) M. Iwasaki, *J. Magn. Resonance* **16** (1974) 417;
- 10) A. Abragam and B. Bleaney, in *Electron Paramagnetic Resonance of Transition Ions*, Ch. 2, Clarendon Press, Oxford, 1970;
- 11) W. Gordy, *Theory and Application of Electron Spin Resonance*, John Wiley&Sons, New York, 1980;
- 12) J. Hüttermann, W. A. Bernhard, E. Haindl and G. Schmidt, *Molec. Phys.* **32** (1976) 1111.

SLABO IZRAŽENE POJAVE U EPR SPEKTRU PARAMAGNETIČNOG
CENTRA SLIČNOG ŠUPLJINI U CITOZIN HIDROKLORIDU

Proučavane su slabo izražene, neredovite pojave u EPR spektrima paramagnetičnog centra sličnog šupljini u ozračenim kristalima citozin hidroklorida s primjesama tiocitozina. Za objašnjenje ponašanja upotrijebljen je spinski Hamiltonijan koji se sastoji od elektronskog Zeemanovog člana, nuklearnog Zeemanovog člana, člana hiperfine i člana kvadrupolne sprege jezgre s elektronom. Pokazano je da kvadrupolni član koji potječe od klora ne samo unosi pomak EPR spektralnih linija, nego uzrokuje i pojavu dodatnih, "zabranjenih" prijelaza. Iz mjerenja slabo izraženih pomaka linija i položaja "zabranjenih" linija izračunat je kvadrupolni tenzor.